Atmos. Chem. Phys. Discuss., 9, 12857–12898, 2009
www.atmos-chem-phys-discuss.net/9/12857/2009/

Atmospheric Chemistry and Physics Discussions

This discussion paper is/has been under review for the journal *Atmospheric Chemistry and Physics (ACP)*. Please refer to the corresponding final paper in *ACP* if available.

Use of a mobile laboratory to evaluate changes in on-road air pollutants during the Beijing 2008 Summer Olympics

M. Wang[1], T. Zhu[1], J. Zheng[2], R. Y. Zhang[2], S. Q. Zhang[1], X. X. Xie[1], Y. Q. Han[1], and Y. Li[3]

[1]State Key Laboratory of Environmental Simulation and Pollution Control, College of Environmental Sciences and Engineering, Peking University, Beijing, 100871, China
[2]Department of Atmospheric Sciences, Texas A&M University, Texas 77843, USA
[3]Chinese Academy of Meteorological Science, Beijing, 100081, China

Received: 12 May 2009 – Accepted: 19 May 2009 – Published: 5 June 2009

Correspondence to: T. Zhu (tzhu@pku.edu.cn)

Published by Copernicus Publications on behalf of the European Geosciences Union.

Abstract

China implemented systematic air pollution control measures during the 2008 Beijing Summer Olympics and Paralympics to improve air quality. This study used an innovative mobile laboratory to conduct in situ monitoring of on-road air pollutants along Beijing's 4th Ring Road on 31 selected days before, during, and after the Olympics air pollution control period. A suite of instruments with response times of less than 30 s was used to measure temporal and spatial variations in traffic-related air pollutants, including NO_x, CO, $PM_{1.0}$ surface area (S_{PM_1}), black carbon (BC), and benzene, toluene, ethylbenzene, and m-, p-, and o-xylene (BTEX). During the Olympics (8–23 August 2008), on-road air pollutant concentrations decreased significantly by up to 54% for CO, 41% for NO_x, 70% for SO_2, 66% for BTEX, 12% for BC, and 18% for S_{PM_1} compared to the pre-control period (before 20 July). Concentrations increased again after the control period ended (after 20 September), with average increases of 33% for CO, 42% for NO_x, 60% for SO_2, 40% for BTEX, 26% for BC, and 37% for S_{PM_1}. Variations in pollutants concentrations were correlated with changes in traffic speed and the number and types of vehicles on the road. Throughout the measurement periods, the concentrations of NO_x, CO, and BTEX varied markedly with the numbers of light- and medium-duty vehicles (LDVs and MDVs, respectively) on the road. Only after 8 August was a noticeable relationship between BC and S_{PM_1} and the number of heavy-duty vehicles (HDVs) found. Additionally, BC and S_{PM_1} showed a strong correlation with SO_2 before the Olympics, indicating possible industrial sources from local emissions as well as regional transport activities in the Beijing area. Such factors were identified in measurements conducted on 6 August in an area southwest of Beijing. The ratio of benzene to toluene, a good indicator of traffic emissions, shifted suddenly from about 0.26 before the Olympics to approximately 0.48 after the Olympics began. This finding suggests that regulations on traffic volume and restrictions on the use of painting solvents were effective after the Olympics began. This study demonstrated the effectiveness of air pollution control measures and identified local and regional pollution

ACPD

9, 12857–12898, 2009

sources within and surrounding the city of Beijing. The findings will be invaluable for emission inventory evaluations and model verifications.

1 Introduction

As the host of the 2008 Summer Olympic Games (the Games of the XXIX Olympiad), Beijing drew international attention for its severe air pollution. Since its economic boost in the early 1980s, Beijing has become a megacity of more than 17 million residents. High energy demands by both domestic and industrial users have led to ever increasing consumption of fossil fuels in the processes of electricity generation, manufacturing, construction, and transportation. In turn, such activities have produced massive emissions of nitrogen oxides (NO_x=NO+NO_2), carbon monoxide (CO), sulfur dioxide (SO_2), volatile organic compounds (VOCs), and particulate matter (PM), including black carbon (BC). The air pollution problems in Beijing are characterized by poor visibility resulting from high mass loading of fine PM (Rogers et al., 2006) and high atmospheric oxidation capability due to photochemical smog formations (Tang, 2004). Recent studies have indicated that both regional and local sources contribute to air pollution events in Beijing, with local sources mainly associated with automobile emissions (Streets et al., 2007). The number of automobiles in Beijing has increased rapidly in recent years at an annual rate of about 15% (Chan et al., 2008; Han et al., 2008). By the year 2020, Beijing is expected to have 5 million automobiles (Hao et al., 2006). Automobiles emit substantial air pollutants into the urban airshed. Liu et al. (2007) estimated that on-road automobiles in Beijing emitted approximately 3 tons of PM, 199 tons of NO_x, 192 tons of VOCs, and 2403 tons of CO daily. Furthermore, chemical mass balance modeling with VOC observations during 2002–2003 showed that automobile exhaust was responsible for 57.7% of the VOC emissions in Beijing (Liu et al., 2005), while 70% of the VOCs in summer were traced back to gasoline-engine vehicles and fugitive gasoline vapors (Liu et al., 2005; Song et al., 2008).

To improve air quality and maintain clean air throughout the Olympic Games, sys-

ACPD
9, 12857–12898, 2009

tematic long- and short-term emission reduction measures and regulations were implemented before and during the Olympic Games, including relocating heavy polluters (e.g., the Capital Steel Company), introducing strict vehicular emissions standards (equivalent to the Euro IV standards), reducing on-road private cars by half during the Olympics period through an odd/even plate number rule, and freezing construction activities during the Olympic Games (The 14th control strategy on Beijing air quality, 2008, available at: http://www.bjepb.gov.cn/bjhb/tabid/68/InfoID/15395/frtid/40/Default.aspx). For the atmospheric chemistry community, these Olympics air quality measures provided a unique opportunity to study the effects of a set of administrative regulations on air quality in a megacity over a relatively short period. To evaluate the effectiveness of the air pollution measures, an international collaborative field campaign, Campaigns of Air quality Research in Beijing and Surrounding Region-2008 (CAREBeijing-2008), was conducted before and during the 2008 Olympics.

As part of CAREBeijing-2008, a mobile research platform was developed and used to provide in situ rapid-response observations of both the spatial and temporal distributions of traffic emissions; such data cannot be obtained by stationary monitoring sites. Relevant studies of real-time measurements have taken place in Europe (Bukowiecki et al., 2002; Weijers et al., 2004; Pirjola et al., 2006), the United States (Kittelson et al., 2004; Jiang et al., 2005; Westerdahl et al., 2005; Rogers et al., 2006; Zavala et al., 2006; Isakov et al., 2007), and Asia, including Hong Kong (Yao et al., 2006, 2007). However, only preliminary studies had been conducted in Beijing (Westerdahl et al., 2009). Most previous studies focused on ultrafine particle (UFP) measurements along motorways, such as “chase studies” for specific vehicle emission factors (Canagaratna et al., 2004; Herndon et al., 2005). Rarely has the use of a mobile laboratory for temporal and spatial analysis been reported.

In this report, we newly present in situ on-road measurements of both gaseous and aerosol phase pollutants in Beijing before, during, and after the 2008 Summer Olympic Games. The temporal and spatial distributions of air pollutants within and around the city were characterized during different stages of the air pollution control measures.

ACPD
9, 12857–12898, 2009

We examined associations of air pollution with meteorological parameters and the influence of different control measures on air pollutant concentrations. The regional transport of SO_2 from the south of Beijing is also discussed. The results of this work demonstrate that a mobile platform is an excellent tool for real-time characterization of on-road air pollution and can provide first-hand evaluations and prompt feedback regarding emission reduction regulations.

2 Experimental methods

2.1 Mobile laboratory platform

An IVECO Turin V diesel vehicle (L=6.6 m, W=2.4 m, H=2.8 m; payload=2.7 metric tons) was selected as the mobile laboratory platform for online instrumentation and for performing on-road measurements (Fig. 1). To ensure the continuous operation of a complete suite of instruments (for measuring both gas- and aerosol-phase species) and to meet the required power consumption of 2.7 kW, two sets of uninterruptible power systems (UPSs) consisting of two series of 12 V/110 Ah lead batteries were deployed and could support all the equipment operations without interruption for up to 6 h. In the case of long-range regional measurements, a 6.5-kW/220 V gasoline-fueled electrical generator could supply power to all the instruments for more than 12 h. Two individual sampling inlet systems were constructed to minimize pollutant loss in the inlet and to enhance the sampling efficiency. The two inlets were located separately at the front top of the van, 3.2 m above the ground; one inlet was for the gaseous pollutant instruments and the other was for the particle instruments. The gaseous pollutant inlet consisted of 1.54-cm outer-diameter (OD) Teflon tubing and a glass manifold to reduce chemical reactions on the sampling walls. For particles, an isokinetic sampling system was designed to minimize aerosol aerodynamic losses. Airflows containing particles were forced horizontally into a cone-shaped stainless steel tube with a total length of 60 cm, an inlet with inner diameter (ID) of 1.4 cm, and a body ID of 9 cm. Then part of

ACPD
9, 12857–12898, 2009

the sample flow was isokinetically fed into a vertically positioned stainless steel tube (ID 1.54 cm) and into the van with a constant flow rate of 3.5 standard liters/min (SLPM); the remaining flow was discarded backward. The inlet system had no pump at the back of the 9-cm tube, making it slightly different from the inlet used in a mobile laboratory previous reported (Bukowiecki et al., 2002). To maintain a constant sampling flow rate, the mobile laboratory was kept at a constant speed of 60 km/h during on-road measurements, when the road conditions permitted. The time delays of the sampling system for gas-phase species and particles were about 8 s and 4 s, respectively.

2.2 Instrumentation on the mobile laboratory

Table 1 provides an overview of all the instruments on board the mobile laboratory, including auxiliary equipment such as meteorological sensors and a global positioning system (GPS). Instruments deployed on the mobile laboratory were mainly research-grade commercial instruments based on well established technology, with an emphasis on high time resolutions. A series of gas analyzers from Ecotech (model 9800sA, Australia) were used to measure NO_x, CO, and SO_2 with detection ranges of 0–500 ppb for NO_x, 0–9.8 ppm for CO, and 0–221.3 ppb for SO_2. All the trace gas instruments were configured by the manufacturer to record data at 1 Hz. Online measurement data were recorded with an industrial personal computer (IPC).

Aromatic VOCs were measured with a compact proton-transfer reaction mass spectrometer (PTR-MS; Ionicon, Austria), as used successfully in Mexico City during the MILAGRO 2006 campaign (Fortner et al., 2009). The working principle of the PTR-MS is based on proton transfer reactions between hydronium ions (H_3O^+) and an analyte with a proton affinity higher than that of water (Lindinger et al., 1998; de Gouw and Warneke, 2007; Fortner et al., 2009). Benzene, toluene, and xylene+ethyl benzene were continuously monitored with the PTR-MS using the selected ion monitoring mode. Background checks were performed automatically once every hour by passing the ambient air through a catalytic converter (de Gouw et al., 2003; Fortner et al., 2009) that could scrub out VOCs without changing the water vapor content. Calibration of the

ACPD
9, 12857–12898, 2009

PTR-MS was conducted using US Environmental Protection Agency TO-15 standards either before or after each on-road sampling trip. The dynamic range of the calibration was from a few to about a hundred parts per billion by volume (ppbv) to accommodate the wide range of on-road air pollutant concentrations.

BC was measured with a multi-angle absorption photometer (MAAP; Thermo model 5012, USA), which utilized a $PM_{2.5}$ cyclone inlet installed in the middle section of the mobile laboratory. The amount of BC was quantified by detecting modifications of the radiation field (670-nm visible light source) in the forward and back hemispheres of a glass-fiber filter caused by BC depositions with a time resolution of 1 min at a flow rate of 16.7 SLPM. The diffusion charging (DC) sensor of the TSI Model 3550 monitor with a high time resolution of 3 s was deployed to measure the corresponding surface area of human lung-depositable particles with a flow rate of 2.5 SLPM. The output data were recorded on an IBM portable PC.

A high-resolution video camera installed atop the mobile laboratory could rotate freely and continuously to provide multi-angle views of on-road conditions and to identify potential emission sources. The Motorola GPS provided precise latitude and longitude data for spatial analysis as well as calculation of moving speed. Both video camera and GPS data were recorded on the IPC.

The Haidian, Chaoyang, and Fengtai meteorological stations of the Chinese Meteorological Administration routinely monitor wind direction (WD) and wind speed (WS). In addition to WD and WS, the Peking University Hospital (PKH) station also monitors relative humidity (RH) and temperature (T). Data from these four stations cover the northwest, east, southwest, and central parts of Beijing and could be used to represent meteorological conditions along the 4th Ring Road.

2.3 Quality assurance and control

Gas-phase instruments were automatically zeroed and calibrated to 80% of the detection range with certified calibration standards (500 ppb NO, accuracy 3%; 9.75 ppm CO, accuracy 3%; and 211.2 ppb SO_2, accuracy 3%; all diluted with N_2, Beijing Huayuan

Gas Chemical Industry Co., Ltd.) before and after each sampling trip. Calibration with five different concentration points (0%, 10%, 20%, 40%, and 80% of the detection range) was performed once every five sampling trips. Difference between the calibration results and the concentrations of standards was less than 4%. VOC measurement uncertainties were determined from variations in the calibration curve slopes and were usually within 20% for each VOC species. The BTEX detection limits were less than 0.3 ppbv, which was three times the standard deviation of the baseline signals. The MAAP and DC were automatically zeroed before the start of each sampling trip. The active surface area concentration calculated from SMPS (Bukowiecki et al., 2002) and the corresponding DC concentration agreed within 95% for these measurements.

Intercomparison was carried out by parking the mobile laboratory on the ground close to the Peking University (PKU) monitoring station, which is approximately 20 m a.g.l. The intercomparison lasted from 24 to 25 August 2008. Differences between gas-pollutant concentrations were found to be within 15%, with correlation coefficients of 0.82, 0.89, and 0.91 for SO_2, NO_x, and CO, respectively. The PTR-MS in the mobile lab and the PTR-MS (Ionicon) at the PKU station agreed in their VOC diurnal variation trends. However, the concentration observed by the PTR-MS at the PKU station was only about 79% of that observed by the mobile lab PTR-MS; this difference may be related to the different elevations of the two monitoring locations.

2.4 Measurement strategy and vehicle traffic speed monitoring

The 4th Ring Road (Fig. 2) was selected as the route for each measurement trip because various types of vehicles are allowed on this road and it has no traffic lights and represents typical major road conditions in Beijing. The 4th Ring Road is 72 km long and encircles the most urban part of Beijing. We conducted measurements in the afternoon because at this time the 4th Ring Road normally has no traffic jams, and the mobile laboratory could keep a relatively constant speed during each sampling trip. Each trip started at 15:30 or 16:00 LT and completed the 4th Ring Road circle within

ACPD
9, 12857–12898, 2009

approximately 70 min; in total, 31 measurement trips were made. To clarify the spatial variation of on-road air pollutants, we divided the 4th Ring Road into north, east, south, and west road sections, which were further equally divided into 16 segments (colored blue and red).

Self-contamination by exhaust from the mobile laboratory could be effectively avoided by using batteries as the instrument power supply and maintaining a constant speed of 60 km/h.

To continuously monitor traffic speed and vehicle numbers on the 4th Ring Road, a Sony video camera mounted on Sijiqing Bridge on the west section of the 4th Ring Road was operated from 17:00 to 18:00 LT for 28 days, corresponding to periods of the research trips. Vehicle types were cataloged into three categories: LDVs, MDVs, and HDVs.

2.5 Air pollution control measures

Table 2 summarizes various air pollution control measures adapted by the Beijing Municipal Environmental Protection Bureau (EPB) at different stages before and during the Olympics.

3 Results and discussion

3.1 Temporal and spatial variations of on-road air pollutants

As shown in Fig. 3, strong temporal and spatial variations in the concentrations of benzene, toluene, BTEX, NO_x, BC, and PM_1 surface area (S_{PM_1}) were measured from 18 July to 6 October in Beijing. The numbers 1, 2, and 3 represent periods of air pollution control measures: e.g., 1, before full-scale control (before 20 July); 2, during full-scale control (20 July–20 September); 3, post-Olympics (after 20 September). The letters N, E, S, and W represent the north, east, south, and west sections of the 4th

ACPD
9, 12857–12898, 2009

Ring Road, respectively. A constant speed of about 60 km/h was maintained during each trip, which took roughly 70 min to complete; each grid therefore represents a 1-min time window and 1 km driving distance on the 4th Ring Road. The blank grids in the figures denote missing data due to technical problems. The sudden changes in color within minutes were associated with air directly emitted from vehicle exhaust.

As shown in Fig. 3, the BTEX concentration was 30 ppb before the full-scale control period; on 22 July, just 2 days after the beginning of the full-scale control, BTEX decreased drastically to about 10.2 ppb and maintained this level until the end of the Olympics, with a level of 7 ppb on 23 August. On 28 and 30 July, BTEX dropped to an average concentration less than 1 ppb, mainly due to rain and wind from the north. After the end of the air pollution control period (20 September), BTEX gradually increased and reached a peak level of 15 ppb (28 September). The NO_x concentration showed a similar trend but increased to a higher level than that of BTEX after the traffic control period ended.

Trends of S_{PM_1} and BC concentrations were similar to those of BTEX and NO_x, with the lowest levels observed during the Olympics period. However, after the air pollution control period, both the PM_1 surface area and BC concentration increased by a factor larger than that of BTEX and close to that of NO_x.

To further evaluate the temporal and spatial variation of on-road pollutants before, during, and after the Beijing Olympics, data were examined from the north, east, south, and west sections of the 4th Ring Road. Figure 4 shows the average concentrations of NO_x, CO, BC, and S_{PM_1} along the four sections during the different air pollution control periods: pre-full-scale control (before 20 July), full-scale control during the Olympics (8–23 August), and post-Olympics (after 20 September). The standard deviations indicate the concentration variations in the four segments, as shown in Fig. 2.

Along the four sections, the average concentrations of NO_x, CO, BETX, SO_2, BC, and S_{PM_1} were all lowest during the Olympics. Among gaseous pollutants and PM, BTEX concentrations showed the largest reduction between the pre-full-scale control period and post-Olympics period. Concentrations of NO_x were similar in the pre-full-scale

ACPD
9, 12857–12898, 2009

control and post-Olympics periods; CO had a lower concentration in the post-Olympics period than during the pre-full-scale control period, while SO_2 and BC concentrations as well as S_{PM_1} had slightly higher values in the post-Olympics period than in the pre-full-scale control period. These differences suggest that the pollutants were influenced by different emission sources and subsequently by different control measures.

During the same periods, no large difference was observed in the average concentrations of on-road air pollutants in the four sections of the 4th Ring Road, suggesting that the air pollutants were homogeneously distributed in Beijing and that the air pollution controls were effective for the whole city. However, in the pre-full-scale control period, concentrations of NO_x, CO, and BTEX and S_{PM_1} showed similar spatial distribution, with the highest values in the north section, followed by the east, south, and west sections. This result probably reflects impacts of the prevailing WD on the dispersion of air pollutants; during the sampling trips, winds were primarily from the south and southwest. Thus, the north and east sections would have been downwind of Beijing and influenced by vehicular emissions from the city, while the south and west sections would have been upwind. During and after the Olympics, this spatial distribution pattern changed, probably due to implementation of the air pollution reduction measures within Beijing during the Olympics as well as a change in wind patterns after the Olympics. The exception of SO_2 in the spatial variation likely reflects the long-distance transport of SO_2 from other areas because no major SO_2 emission source exists within the city of Beijing.

3.2 Influence of meteorological conditions on air pollutants

Given that meteorological conditions also influence the concentrations of gaseous pollutants and PM, we additionally assessed the influence of WS, WD, RH, and T on air pollutant concentrations. Figure 5 presents a rose plot of WS and WD in Beijing from 15:30 to 17:00 LT on the days of our sampling trips. These results confirm that wind patterns were consistent at different stations in Beijing, with prevailing winds from the south, southwest, and northeast. With low WS (<2 m s^{-1}), more fluctuation in WD was

ACPD
9, 12857–12898, 2009

observed.

Table 3 shows the correlation coefficients between the concentrations of air pollutants averaged over each road segment and the meteorological parameters (WS, T, RH) measured at the PKH station throughout the campaign. We used PKH data because this station is located at the center of Beijing. Generally, WS and T showed slightly negative correlations with the concentrations of all the selected pollutants, similar to the results reported by Akpinar et al. (2008). Meanwhile, the concentrations of air pollutants showed slight positive correlations with RH. Although no pronounced correlation was found within the whole measurement period, certain meteorological conditions unfavorable for pollutant dispersion may have led to high levels of air pollution. For example, on 4 August, SO_2 and BC concentrations and S_{PM_1} increased rapidly to 17.3 ppb, 7.27 μg/m^3 and 122.5 μm^2/cm^3, respectively, concurrent with high RH and low WS.

Figure 6 shows the correlations between benzene concentrations averaged for each segment and RH and T in the pre-, control, and post-control periods. By selecting the high-frequency distributions of RH and T among the whole data, the ranges in RH and T were chosen as 35–62% and 25–35°C, respectively. The benzene concentrations had weak positive correlations with RH and negative correlations with T. However, benzene concentrations varied in different periods; before the Olympics, benzene varied from 4 to 6 ppb within a RH range of 50–60% and T range of 30°C–32°C; this was much higher than the values of 0–3 ppb during and after the Olympics within the same RH and T ranges. This large difference clearly indicates that the emission control measures were very effective in reducing on-road concentrations of benzene.

3.3 Effectiveness of the measures on reducing air pollutants

3.3.1 Traffic-related air pollutants

Most of the CO, NO_x, BTEX, fine particles, and BC measured in this study were likely from motor vehicle emissions, which previous studies have estimated as accounting

ACPD
9, 12857–12898, 2009

for 74% of the NO_x and 57.7% of VOCs emitted in Beijing (Hao et al., 2005; Liu et al., 2005). Both CO and NO_x are commonly used as traffic emission indicators. We can thus expect that the on-road concentrations of these pollutants will be correlated with each other. Table 4 shows significant positive correlations between the average concentrations of CO and BTEX and of NO_x and BTEX. The concentrations were averaged over each of the 16 segments of the 4th Ring Road throughout the whole campaign. Correlation coefficients ranged from 0.66 to 0.76 for CO and BTEX and from 0.60 to 0.70 for NO_x and BTEX. Benzene is a marker of volatile aromatic hydrocarbons in regions of intensive traffic (Khoder, 2007). In this study, benzene displayed strong correlations (r>0.86) with other BTEX species, indicating that vehicular sources mainly controlled BTEX concentrations. Given that emissions from LDVs with gasoline engines have been identified as the major portion of the total vehicular emissions in Beijing (Hao et al., 2005; Song et al., 2007), concentrations of on-road air pollutants (e.g., CO, NO_x, and BTEX species) should be well correlated with the number of LDVs on the road, as will be discussed in a later section.

While S_{PM_1} and BC showed a good association with each other (r=0.7), they correlated weakly with CO and NO_x (r<0.43). Combustion sources such as vehicles, power plants, and biomass burning emit BC, and S_{PM_1} can serve as an indicator for fine particles. The correlation between S_{PM_1} and BC in this study indicated that on-road fine particles and BC came from similar sources. The weak correlation between BC and CO and NO_x as well as between S_{PM_1} and CO and NO_x suggests BC and S_{PM_1} in Beijing have sources other than LDVs. Since industrial activities have been slow down and biomass combustion were strictly prohibited in Beijing during the Olympics, BC and S_{PM_1} could have been generated by HDVs with diesel engines (Fruin et al., 2004; de Castro et al., 2008), even though HDV exhaust does not constitute a major portion of overall traffic exhaust in Beijing.

ACPD
9, 12857–12898, 2009

3.3.2 Association between on-road air pollutants and number of vehicles

Different air pollution control measures were implemented at different stages of the Olympics. To evaluate the effects of various control measures on reducing air pollution in Beijing, we divided the data set into the following seven periods covering both the Olympics and Paralympics periods: 1, before full-scale control (before July 20); 2, full-scale control before the Olympics (20 July–7 August 2008); 3, full-scale control during the Olympics (8–23 August 2008); 4, between the Olympics and the Paralympics (24 August–6 September 2008); 5, full-scale control during the Paralympics (7–19 September 2008); 6, post-Olympics (20–27 September 2008); and 7, national holidays (28 September–4 October 2008). Table A1 provides detailed information about the sampling trips, average concentrations of air pollutants over these periods, and observed vehicle numbers, categorized as LDVs, MDVs, and HDVs.

Figure 7a and b shows the average concentrations of NO_x, CO, and BTEX concentrations in these different controlling periods, and the concurrent numbers of LDVs and MDVs per hour; Fig. 7c shows the BC concentration and S_{PM_1} with the number of HDVs per hour. The standard deviations represent the concentration variation of those pollutants during each sampling trip within corresponding periods.

Pollutant concentrations varied widely by period according to policy alterations and appeared to be strongly influenced by traffic density. Before full-scale traffic control (before 20 July), NO_x, CO, and BTEX concentrations had identical patterns, reaching peak values of 110.8±30.0 ppb for NO_x, 2.4±0.7 ppm for CO, 3.4±3.0 ppb for benzene, 7.4±3.4 ppb for toluene, and 10.4±4.7 ppb for X+E, respectively., respectively. Under the strictest vehicle restrictions during the Olympics (8–23 August), each of these species reached its lowest concentrations recorded during this study. After the Olympics, the average values of these species increased again. These trends correspond to those in the numbers of LDVs and MDVs per hour on the 4th Ring Road. This result is consistent with the assumption that gasoline-fueled LDVs and MDVs are the main sources of NO_x, CO, and BTEX in Beijing. Apparently, controlling the number

ACPD
9, 12857–12898, 2009

of LDVs and MDVs on the road was very effective in reducing NO_x, CO, and BTEX concentrations.

Furthermore, during the Olympics and the periods thereafter, the BC concentration and S_{PM_1} showed increasing trends similar to those in the number of HDVs. This finding suggests that diesel-powered HDVs may be major sources of on-road BC and fine particles. However, before the Olympics period, the changes in BC concentration and S_{PM_1} did not closely follow the change in HDV number, indicating that before the Olympics, other emission sources, such as industry emission and biomass burning, also contributed to on-road fine particles and BC.

3.4 Sources of SO_2, BC, and S_{PM_1}

BC and S_{PM_1} have weak correlations with CO and NO_x, with correlation coefficient $r<0.43$ (Table 4), while their correlation with SO_2 was stronger ($r>0.45$). This suggests that regional transport might also play a role in contributing on-road fine particles, since the SO_2 was strictly regulated in Beijing and mainly come from sources outside Beijing.

Further information about the sources of fine particles can be found in Fig. 7c, which shows BC concentration and S_{PM_1} correlated with the number of HDVs differently in the periods before and after 8 August. After 8 August, both BC concentration and S_{PM_1} follow the trend of HDVs numbers well. This indicates that BC and on-road fine particles came from different sources in these two periods. Although BC data were recorded on only one day during the period of 20 July to 7 August, the same type of instrument at a ground-based station displayed a trend of BC concentrations similar to that illustrated in Fig. 7c.

To identify the underlying causes of the observed patterns of BC and S_{PM_1}, we divided the periods into before and after 8 August to examine correlations between BC and S_{PM_1} with NO_x, CO, BTEX, and SO_2. As shown in Table 5, before 8 August, BC and S_{PM_1} had weak correlations with BTEX ($r<0.23$), NO_x ($r<0.31$), and CO ($r<0.41$), but strong associations with SO_2 ($r>0.86$). However, after 8 August, higher correlations of BC and S_{PM_1} to BTEX ($r>0.52$), NO_x ($r>0.60$), and CO ($r>0.63$) were observed,

ACPD
9, 12857–12898, 2009

while the correlation coefficient of SO_2 to BC and S_{PM_1} declined to less than 0.52. This difference indicates that, before 8 August, BC, fine particles, and SO_2 were very likely from similar sources, most likely from emissions by industrial and power plant sources; after 8 August, under stricter regulations, the main sources that emitted both BC, fine particles, and SO_2 were effectively controlled, while the strong correlations of NO_x, CO, and BTEX between BC and S_{PM_1} suggests that BC and S_{PM_1} were mainly come from vehicular sources, most likely HDVs with diesel-fueled engine.

3.5 BTEX: vehicular emissions versus paints and solvents

The benzene/toluene ratio (B/T) is a key indicator of aromatics originating predominantly from vehicle emissions (Beauchamp et al., 2004; Hoque et al., 2008). This ratio is useful for estimating the photochemical age of an air mass (Khoder, 2007) and is therefore another indicator of the effectiveness of traffic control measures. The atmospheric lifetimes for benzene and toluene have been estimated as 9.4 and 1.9 days, respectively, due to their reactions with OH (Atkinson, 2000). The B/T is normally the same in urban areas, ranging from 0.25 to 0.5 and usually around 0.5 when vehicle emissions are the primary sources (Perry and Gee, 1995; Brocco et al., 1997; Barletta et al., 2005). The rapid response of the PTR-MS allowed us to observe real-time variation in the B/T, as is shown in Fig. 8. The large fluctuation in the B/T in Fig. 8 is due to the high time resolution of the PTR-MS (30 s), which allows it to record emission plumes and reflect traffic-related factors such as traffic density, vehicle types, fuel composition, and fresh exhausts from vehicles directly in front of the mobile laboratory.

Before 4 August, B/T values were low and highly variable with an average value of 0.26±0.06. In contrast, higher B/T with less fluctuation was observed after 12 August, when the average value was 0.48±0.07. Benzene and toluene are emitted in vehicle exhaust and gasoline evaporation, while toluene is also released from the use of solvents (e.g., painting, printing, and dry cleaning activities) (Na et al., 2003), whose evaporations are closely dependent on ambient temperature (Schnitzhofer et al., 2008). This suggests that the lower B/T before 4 August may have been caused by the heavy

use of painting solvents for decorating projects in preparation for the Olympics as well as fugitive gasoline emissions containing more toluene than benzene. However, after 12 August, with decorations complete and rigorous controls on solvent usage in place, toluene emissions from paints and solvents became less important than those from vehicular sources, and the B/T was mainly controlled by vehicle emissions.

Studies earlier in this century have examined traffic-related BTEX behaviors in the city of Beijing (Barletta et al., 2005; Song et al., 2007; Wei et al., 2007). However, most of these studies were based on roadside measurements with gas chromatography/mass spectrometry (GC-MS) or GC-flame ionization detector (FID) techniques. Table 6 compares the B/T values obtained from previous studies at the same location or with a similar method. Barletta et al. (2005) reported VOC concentrations in 43 cities of China in 2001 and defined Beijing as a "traffic-related city" for its B/T of 0.6±0.2. Wei et al. (2007) found values of 0.49–0.55, a range similar to ours, from roadside measurements along the 4th Ring Road. A higher value was calculated by Song et al. (2007) at the fixed PKU site 100 m from a main road. In short, previous studies generally reported higher B/T values than ours. The B/T is considered to increase with increasing distance from the pollution source (Gelencser et al., 1997; Simon et al., 2004). Apparently, our mobile laboratory with PTR-MS measured vehicular exhaust at the shortest distance from its sources.

3.6 Local emission and regional transport of SO_2

Several studies on SO_2 transport around Beijing predicted that high SO_2 concentrations will be trapped and accumulate when prevailing winds are from the south or southwest (Sun et al., 2006; Wang et al., 2008), accounting for nearly 23% of the total SO_2 concentration (Zhang et al., 2004). Most of these studies were based on model stimulation and stationary measurements, and real-time regional observation is needed to validate these results.

As shown in Fig. 4, we found higher SO_2 concentration on the south side of the 4th Ring Road than in the other directions, indicating possible transport of SO_2 from the

south. To identify the sources accounting for the high SO_2 values observed from 28 July to 4 August (see Table A1), the mobile laboratory was driven to the southwest of Beijing outside the 4th Ring Road on 6 August; prevailing winds were from the south-southwest and south. As shown in Fig. 9a, the SO_2 concentration in the southern section was higher than that in the northern area. An increase in SO_2 concentration was observed when the mobile laboratory reached Shijingshan district (Fig. 9b) and continued along Jingkai Highway and South 6 Ring Road, where concentrations were 15 ppb. The peak value exceeded 18 ppb on Jiangshi Highway. This maximum then dropped dramatically below 10 ppb when we passed Shijingshan district again on the return trip to PKU.

This trend was consistent with low frequency variations in NO_x concentrations and S_{PM_1}, indication they were from similar combustion sources. The spikes in NO_x concentration and S_{PM_1} during the sampling trip reflected immediate exhaust from nearby traffic, especially at the start of the trip in the northern area near the PKU site, while background increases with broad peaks in NO_x concentrations and S_{PM_1} reflected local or regional transport plumes. Peak values of SO_2, NO_x, and S_{PM_1} in Shijingshan district were likely from local industrial sources within a short distance from the road (approximately 12 km); in contrast, along Jingshi Highway, the peaks likely reflect sources over a wider range (30 km), indicating regional transport.

4 Conclusions

As demonstrated in this study, the mobile laboratory was a useful tool for directly evaluating changes in on-road air pollutants along Beijing's 4th Ring Road associated with short-term pollution controls for the Beijing 2008 Summer Olympics. The mobile laboratory collected data that could not have been obtained through stationary observations.

We conducted repeat measurements on 31 days from 18 July to 6 October 2008, covering periods before, during, and after the Olympics pollution controls. Our results

ACPD
9, 12857–12898, 2009

show that the emission control measures were effective in reducing on-road air pollutants.

High correlations among NO_x, CO, and BTEX species were observed, indicating that the their dominant source was gasoline exhaust from LDVs and MDVs. High correlations were also identified between BC and PM_1 surface area, suggesting that HDV diesel exhaust was a major source when other BC and PM_1 sources were strictly controlled during the Olympics period. Concentrations of NO_x, CO, and BTEX deceased dramatically from extremely high values before traffic control regulations to their lowest concentrations during the Olympic periods. However, concentrations then increased gradually after the Olympic regulations, especially after the traffic control period, and varied consistently with LDV and MDV traffic-speed variations. No discernible declines in BC and PM_1 surface area were observed before the Olympics, while gradual increases were shown afterward, corresponding to the number of HDVs on-road.

The strong relationship of BC and S_{PM_1} with SO_2 found before the Olympics (before 8 August) indicated that they had similar local emissions or regional transport sources, which were later controlled. This suggestion was later demonstrated by the mobile monitoring in the southwest area outside Beijing on 6 August, when complicated SO_2 sources both from local emissions and regional transport were identified.

The B/T, regarded as a source indicator, was 0.26±0.06 before 8 August but 0.48±0.07 in the periods after 8 August. This difference points to the heavy use of painting solvents in Beijing before the Olympics (before 8 August) and the traffic speed and types after 8 August when pre-Olympics decorations were completed and rigorous controls were placed on solvent usage. With painting solvents becoming less important, the B/T reached a value mainly controlled by vehicle emissions.

Therefore, our mobile laboratory successfully demonstrated that the control strategies implemented by the Beijing EPB were effective in improving air quality within a short term. Further studies on regional sources of both SO_2 and PM on different ring roads of Beijing City as well as areas south of Beijing are needed in the future.

ACPD
9, 12857–12898, 2009

Appendix A

Supporting information

Please, see Table A1 for further information.

Acknowledgements. This study was supported by Beijing Environmental Protection Bureau (OITC-G08026056). We would like to thank TSI Inc. for their assistance on PM_1 surface area instrument support. Special thanks also to Chinese Meteorological Administration for meteorological data support. We also thank to Min Shao and Ying Liu for assistance in PTR-MS inter-comparison.

References

Akpinar, S., Oztop, H. F., and Akpinar, E. K.: Evaluation of relationship between meteorological parameters and air pollutant concentrations during winter season in Elazg, Turkey, Environ. Monit. Assess., 146, 211–224, 2008.

Atkinson, R.: Atmospheric chemistry of VOCs and NO_x, Atmos. Environ., 34, 2063–2101, 2000.

Barletta, B., Meinardi, S., Rowland, F. S., Chan, C. Y., Wang, X., Zou, S. C., Chan, L. Y., and Blake, D. R.: Volatile organic compounds in 43 Chinese cities, Atmos. Environ., 39, 5979–5990, 2005.

Beauchamp, J., Wisthaler, A., Grabmer, W., Neuner, C., Weber, A., and Hansel, A.: Short-term measurements of CO, NO, NO_2, organic at a motorway locationcompounds and PM_{10} in an Austrian valley, Atmos. Environ., 38, 2511–2522, 2004.

Brocco, D., Fratarcangeli, R., Lepore, L., Petricca, M., and Ventrone, I.: Determination of aromatic hydrocarbons in urban air of Rome, Atmos. Environ., 31, 557–566, 1997.

Bukowiecki, N., Dommen, J., Prévôt, A. S. H., Richter, R., Weingartner, E., and Baltensperger, U.: A mobile pollutant measurement laboratory-measuring gas phase andaerosol ambient concentrations with high spatial and temporal resolution, Atmos. Environ., 36, 5569–5579, 2002.

Canagaratna, M. R., Jayne, J. T., Ghertner, D. A., Herndon, S., Shi, Q., Jimenez, J. L., Silva, P. J., Williams, P., Lanni, T., Drewnick, F., Demerjian, K., Kolb, C. E., and Worsnop, D. R.: Chase Studies of Particulate Emissions from in-use New York City Vehicles, Aerosol Sci. Technol., 38(6), 555–573, 2004.

Chan, C. K. and Yao, X. H.: Air pollution in mega cities in China, Atmos. Environ., 42, 1–42, 2008.

de Gouw, J. A. and Warneke, C.: Measurment of volatile organic compounds in the earth's atmosphere using proton-transfer-reaction mass spectrometry, Mass Spectrom. Rev., 26, 223–257, 2007,

de Gouw, J. A., Goldan, P. D., Warneke, C., Kuster, W. C., Roberts, J. M., Marchewka, M., Bertman, S. B., Pszenny, A. A. P., and Keene, W. C: Validation of proton transfer reaction-mass spectrometry (PTR-MS) measurements of gas-phase organic compounds in the atmosphere during the New England Air Quality Study (NEAQS) in 2002, J. Geophys. Res., 108(D21), 4682, doi:10.1029/2003JD003863, 2003.

de Castro, B. R., Wang, L., Mihalic, J. N., Breysse, P. N., Geyh, A. S., and Buckley, T. J.: The Longitudinal Dependence of Black Carbon Concentration on Traffic Volume in an Urban Environment, J. Air Waste Manage., 58, 928–939, 2008.

Fortner, E. C., Zheng, J., Zhang, R., Berk Knighton, W., Volkamer, R. M., Sheehy, P., Molina, L., and André, M.: Measurements of Volatile Organic Compounds Using Proton Transfer Reaction - Mass Spectrometry during the MILAGRO 2006 Campaign, Atmos. Chem. Phys., 9, 467–481, 2009, http://www.atmos-chem-phys.net/9/467/2009/.

Fruin, S. A., Winer, A. M., and Rodes, C. E.: Black carbon concentrations in California vehicles and estimation of in-vehicle diesel exhaust particulate matter exposures, Atmos. Environ., 38, 4123–4133, 2004,

Gelencser, A., Siszler, K., and Hlavay, J.: Toluene-Benzene concentration ratio as a tool for characterizing the distance from vehicular emission sources, Environ. Sci. Technol., 31, 2869–2872, 1997.

Han, J. and Hayashi, Y.: Assessment of private car stock and its environmental impacts in China from 2000 to 2020, Transport. Res. D-Tr. E., 13, 471–478, 2008.

Hao, J. M. and Wang, L. T.: Improving Urban Air Quality in China: Beijing Case Study, J. Air Waste Manage., 55, 1298–1305, 2005.

Hao, J. M., Hu, J. N., and Fu, L. X.: Controlling vehicular emissions in Beijing during the last decade, Transpor. Res.A-Pol., 40, 639–651, 2006.

Herndon, S. C., Jayne, J. T., Zahniser, M. S., Worsnop, D. R., Knighton, B., Alwine, E., Lamb, B. K., Zavala, M., Nelson, D. D., McManus, J. B., Shorter, J. H., Canagaratna, M. R., Onasch, T. B., and Kolb, C. E.: Characterization of urban pollutant emission fluxes and ambient concentration distributions using a mobile laboratory with rapid response instrumentation, Faraday Discuss., 130, 327–339, 2005.

Hoque, R. R., Khillare, P. S., Agarwal, T., Shridhar, V., and Balachandran, S.: Spatial and temporal variation of BTEX in the urban atmosphere of Delhi, India, Sci. Total Environ., 392, 30–40, 2008.

Isakov, V., Touma, J. S., and Khlystov, A.: A Method of Assessing Air Toxics Concentrations in Urban Areas Using Mobile Platform Measurements, J. Air Waste Manage., 51, 1286–1295, 2007.

Jiang, M., Marr, L. C., Dunlea, E. J., Herndon, S. C., Jayne, J. T., Kolb, C. E., Knighton, W. B., Rogers, T. M., Zavala, M., Molina, L. T., and Molina, M. J.: Vehicle fleet emissions of black carbon, polycyclic aromatic hydrocarbons, and other pollutants measured by a mobile laboratory in Mexico City, Atmos. Chem. Phys., 5, 3377–3387, 2005, http://www.atmos-chem-phys.net/5/3377/2005/.

Khoder, M. I.: Ambient levels of volatile organic compounds in the atmosphere of Greater Cairo, Atmos. Environ., 41, 554–566, 2007.

Kittelson, D. B., Watts, W. F., and Johnson, J. P.: Nanoparticle emissions on Minnesota highways, Atmos. Environ., 38, 9–19, 2004.

Kolb, C. E., Herndon, S. C., McManus, J. B., Shorter, J. H., Zahniser, M. S., Nelson, D. D., Jayne, J. T., Canagaratna, M. R., and Worsnop, D. R.: Mobile Laboratory with Rapid Response Instruments for Real-Time Measurements of Urban and Regional Trace Gas and Particulate Distributions and Emission Source Characteristics, Environ. Sci. Technol., 38, 5694–5703, 2004.

Lindinger, W., Hansel, A., and Jordan, A.: On-line monitoring of volatile organic compounds at pptv levels by means of proton-transfer-reaction mass spectrometry (PTR-MS) – Medical applications, food control and environmental researchenvironmental research, Int. J. Mass Spectrom., 173, 191–241, 1998.

Liu, H., He, K. B., Wang, Q. D., Huo, H., Lents, J., Davis, N., Nikkila, N., Chen, C. H., Osses, M., and He, C. Y.: Comparison of Vehicle Activity and Emission Inventory between Beijing and Shanghai, J. Air Waste Manage., 57, 1172–1177, 2007.

Liu, Y., Shao, M., Zhang, J., Fu, L., and Lu, S.: Distributions and source apportionment of

ambient volatile organic compounds in Beijing city, China, in: Proceeding of 2nd International Conference on Environmental Concerns, Xiamen, China, 12–15 October 2004, 1843–1860, 2005.

Na, K., Kim, Y. P., Moon, I., and Moon, K. C.: Diurnal characteristics of volatile organic compounds in the Seoul atmosphere, Atmos. Environ., 37, 733–742, 2003.

Perry, R. and Gee, I. L.: Vehicle emissions in relation to fuel composition, Sci. Total Environ., 169, 149–156, 1995.

Pirjola, L., Paasonen, P., Pfeiffer, D., Hussein, T., Hameri, K., Koskentalo, T., Virtanen, A., Ronkko, T., Keskinen, J., Pakkanen, T. A., and Hillamo, R. E.: Dispersion of particles and trace gases nearby a city highway: Mobile laboratory measurements in Finland, Atmos. Environ., 40, 867–879, 2006.

Rogers, T. M., Grimsrud, E. P., Herndon, S. C., Jayne, J. T., Kolb, C. E., Allwine, E., Westberg, H., Lamb, B. K., Zavala, M., Molina, L. T., Molina, M. J., and Knighton, W. B.: On-road measurements of volatile organiccompounds in the Mexico City metropolitan area using proton transfer reaction mass spectrometry, Int. J. Mass Spectrom., 252, 26–37, 2006.

Schnitzhofer, R., Beauchamp, J., Dunkl, J., Wisthaler, A., Weber, A., and Hansel, A. : Long-term measurements of CO, NO, NO_2, benzene, toluene and PM_{10} at a motorway location in an Austrian valley, Atmos. Environ., 42, 1012–1024, 2008.

Simon, V., Baer, M., Torres, L., Olivier, S., Meybeck, M., and Della-Massa, J. P.: The impact of reduction in the benzene limit value in gasoline on airborne benzene, toluene and xylenes levels, Sci. Total Environ., 334–335, 2004.

Song, Y., Dai, W., Shao, M., Liu, Y., Lu, S. H., Kuster, W., and Goldan, P.: Comparison of receptor models for source apportionment of volatile organic compounds in Beijing, China, Environ. Pollut., 156, 174–183, 2008.

Song, Y., Shao, M., Liu, Y., Lu, S. H., Kuster, W., Goldan, P., and Xie, S. D.: Source Apportionment of Ambient Volatile Organic Compounds in Beijing, Environ. Sci. Technol, 41, 4348–4353, 2007.

Streets, D. G., Fu, J. S., Jang, C. J., Hao, J. M., He, K. B., Tang, X. Y., Zhang, Y. H., Wang, Z. F., Li, Z. P., Zhang, Q., Wang, L. T., Wang, B. Y., and Yu, C.: Air quality during the 2008 Beijing Olympic Games, Atmos. Environ., 41, 480–492, 2007.

Sun, Y., Wang, Y. S., Liu, G. R., An, J. L., Ma, Z. Q., Shi, L. Q., and Xu, H. H.: Analysis for vertical profile of atmospheric SO_2 during air seriously polluted days in Beijing, Environ. Sci., 27, 408–414, 2006 (in Chinese with Abstract in English).

ACPD

9, 12857–12898, 2009

Tang, X.: The characteristics of urban air pollution in China. Urbanization, Energy, and Air Pollution in China, edited by: Fritz, J. J., Washington, DC, The National Academies Press, 47–54, 2004.

Wang, S. L., Xie, P. H., Hu, S. X., Wei, H. L., Hu, H. L., Xie, J., Cao, K. F., and Fang, X.: Measurement of Atmospheric Boundary Layer Pollutants by Mobile Lidar in Beijing, Environ. Sci., 29, 562–568, 2008 (in Chinese with Abstract in English).

Wei, S. F., Teng, M., Fu, Q., and Zhang, Y.: Pollution Characteristic and Source Analysis of BTEX in Ambient Air of Olympic Gymnasium before and after Traffic Restriction, Environmental Monitoring in China, 23, 48–52, 2007 (in Chinese with Abstract in English).

Weijers, E. P., Khlystov, A. Y., Kos, G. P. A., and Erisman, J. W.: Variability of particulate matter concentrations along roads and motorways determined by a moving measurement unit, Atmos. Environ., 38, 2993–3002, 2004.

Westerdahl, D., Fruin, S., Sax, T., Fine, P. M., and Sioutas, C.: Mobile platform measurements of ultrafine particles andassociated pollutant concentrations on freeways and residential streets in Los Angeles, Atmos. Environ., 39, 3597–3610, 2005.

Westerdahl, D., Wang, X., Pan, X. C., and Zhang, K. M.: Characterization of on-road vehicle emission factors and microenvironmental air quality in Beijing, China, Atmos. Environ., 43, 697–705, 2009.

Yao, X. H., Lau, N. T., Chan, C. K., and Fang, M.: Size distributions and condensation growth of submicron particles in on-road vehicle plumes in Hong Kong, Atmos. Environ., 41, 3328–3338, 2007.

Yao, X. H., Lau, N. T., Fang, M., and Chan, C. K.: On the time-averaging of ultrafine particle number size spectra in vehicular plumes, Atmos. Chem. Phys., 6, 4801–4807, 2006, http://www.atmos-chem-phys.net/6/4801/2006/.

Zavala, M., Herndon, S. C., Slott, R. S., Dunlea, E. J., Marr, L. C., Shorter, J. H., Zahniser, M., Knighton, W. B., Rogers, T. M., Kolb, C. E., Molina, L. T., and Molina, M. J.: Characterization of on-road vehicle emissions in the Mexico City Metropolitan Area using a mobile laboratory in chase and fleet average measurement modes during the MCMA-2003 field campaign, Atmos. Chem. Phys., 6, 5129–5142, 2006, http://www.atmos-chem-phys.net/6/5129/2006/.

Zhang, Z. G., Gao, Q. X., Han, X. Q., and Zheng, X. J.: The Study of Pollutant Transport between the Cities in North China, Research of Environmental Sciences, 17, 14–20, 2004 (in Chinese with Abstract in English).

Table 1. Instrumentation deployed on the PKU mobile laboratory.

Parameter	Instrument method/type	Time resolution	Detection limit
Aerosols			
Size distribution D=15–673 nm	Scanning mobility particle sizer (SMPS)/TSI DMA3081, CPC3772	2 min	Not defined
Size distribution D=0.3–20 μm	Optical particle counter(OPC)/Grimm Dust monitor 1.108	6 s	1 particle/l
Active surface area	Diffusion charging sensor(DC)/TSI 3550	3 s	0.1 $\mu m^2/cm^3$
Black carbon	Multi Angle Absorption Photometer(MAAP)/Thermo Model 5012	1 min	0.1 $\mu g/m^3$
Gas phase			
O_3	Ozone analyzer(UV absorption)/ECOTECH 9810A	1 s	0.4 ppb
NO_x	NO_x analyzer(chemiluminescence)/ECOTECH 9841A	1 s	0.4 ppb
CO	CO analyzer(NDIR Gas Filter Correlation)/ECOTECH 9830A	1 s	40 ppb
CO_2	CO_2 analyzer(NDIR Gas Filter Correlation)/ECOTECH 9820A	1 s	2.0 ppm
SO_2	SO_2 analyzer(fluorescence)/ECOTECH 9850A	1 s	0.4 ppb
VOC_s	Proton Transfer Reaction Mass Spectrometry(PTR-MS)/Ionicon	30 s/cycle	<0.3 ppb
Others			
GPS	MOTOROLA FS ONCORE	1 s	Common standard
Temperature	Met One	<1 min	Common standard
Pressure	Met One	<1 min	Common standard
Relative humidity	Met One	<1 min	Common standard
Wind speed/direction	Met One	<1 min	Common standard

ACPD
9, 12857–12898, 2009

Table 2. Starting dates of different air pollution control measures before and during 2008 Olympics (compiled from Beijing EPB released information on web page).

Starting dates	Control measures
1 Jan 2008	Introduce new vehicular emission standard, equivalent to Euro IV
Before	Relocating heavy industrial polluters, install desulfurization facility
31 Jun 2008	Implementing low fugitive emission facilities at more than 1000 gas stations
23 Jun 2008	50% of government cars were not allowed driving on road Diesel and heavy polluted vehicles not allowed driving into Beijing Only the vehicles met emission standard equivalent to Euro II were allows entering in Beijing
20 Jul 2008	Starting the full scale control The odd/even plate number rule for traffic control Stricter control on vehicles entering in Beijing Reduce and stop production at some factories surrounding Beijing
8 Aug 2008	Extra 20% of governmental cars were not allowed driving on road Stop outdoor construction activities Temporally closing some gas stations Increasing bus fleet and transit frequency
20 Sep 2008	Lifting regulations adapted from July 20 Control 20% of private cars based on the last digital of plate number

ACPD
9, 12857–12898, 2009

Table 3. Correlations coefficients (r) between air pollutants and wind speed (WS), temperature (T), and relative humidity (RH).

	CO N=193	NO_x N=201	SO_2 N=203	Benzene N=218	Toluene N=218	X+E N=218	BC N=182	$S^a_{PM_1}$ N=159
WS	−0.03	−0.05	−0.06	−0.11	−0.11	−0.11	−0.05	0.21*
T	0.07	−0.44**	−0.01	−0.28*	−0.35**	−0.35**	−0.30**	−0.31**
RH	0.39**	−0.06	0.41**	0.36**	0.11	0.19*	0.36**	0.04

* Correlation is significant at the 0.05 level (2-tailed). ** Correlation is significant at the 0.01 level (2-tailed). [a] S_{PM_1}: PM_1 surface area.

Table 4. Correlations coefficients (r) between on-road air pollutants measured pre (before 20 July), during (20 July–19 September), and post (after 20 September) traffic control periods.

	CO N=153	NO_x N=131	SO_2 N=143	Benzene N=149	Toluene N=149	X+E N=149	$S^a_{PM_1}$ N=101	BC N=121
CO	1							
NO_x	0.70**	1						
SO_2	0.65**	0.18	1					
Benzene	0.66**	0.60**	0.34**	1				
Toluene	0.75**	0.68**	0.23**	0.88**	1			
X+E	0.76**	0.67**	0.20*	0.86**	0.93**	1		
$S^a_{PM_1}$	0.35**	0.30*	0.45**	0.25*	0.19	0.18	1	
BC	0.43**	0.31**	0.54**	0.34**	0.20*	0.22*	0.70**	1

* Correlation is significant at the 0.05 level (2-tailed). ** Correlation is significant at the 0.01 level (2-tailed). [a] S_{PM_1}: PM_1 surface area.

Table 5. Correlations coefficients (r) between BC and PM_1 surface area (S_{PM_1}) and gaseous pollutants measured pre-Olympics (18 July–8 August), and during Olympics and Paralympics (8 August–19 September).

		Benzene	Toluene	X+E	NO_x	CO	SO_2
18 July–8 August	BC	0.19	0.13	0.10	0.27*	0.41**	0.91**
	S_{PM_1}	0.23*	0.16	0.11	0.31*	0.33*	0.86**
8 August–19 September	BC	0.59**	0.56**	0.52**	0.60**	0.66**	0.52**
	S_{PM_1}	0.60**	0.59**	0.57**	0.64**	0.63**	0.32*

* Correlation is significant at the 0.05 level (2-tailed). ** Correlation is significant at the 0.01 level (2-tailed).

ACPD
9, 12857–12898, 2009

Table 6. Comparisons of benzene/toluene ratio (B/T) from present study and previous references.

B/T ratio	Location	Year	References	Method
0.60±0.20	Beijing	2001	Barletta et al.	Roadside, GC-FID/MS
0.58	Beijing, PKU site	2007	Song et al.	Station, GC-FID/MS
0.49~0.55	Beijing, the 4th Ring Road	2007	Wei et al.	Roadside, GC-MS
0.48±0.07	Beijing, the 4th Ring Road	2008	This study	Mobile monitoring, PTR-MS

ACPD
9, 12857–12898, 2009

Table A1. Average values of selected air pollutants during categorized periods.

Periods	Sampling dates		CO (ppm)	NO_x (ppb)	SO_2 (ppb)	Benzene (ppb)	Toluene (ppb)	*X+E (ppb)	S_{PM_1} ($\mu m^2/m^3$)	BC ($\mu g/m^3$)
Before full scale control (Pre–20 Jul 2008)	18 Jul 2008, 19 Jul 2008	Mean	2.4	147.4	10.2	3.4	7.4	10.4	88.0	6.3
		SD**	0.7	36.1	4.2	3.0	3.4	4.7	16.6	2.2
Full scale control: before Olympics (20 Jul 2008–7 Aug 2008)	22 Jul 2008, 26 Jul 2008, 28 Jul 2008, 30 Jul 2008, 4 Aug 2008	Mean	1.8	107.6	13.0	1.8	4.1	4.5	98.0	7.3
		SD**	0.2	12.0	3.8	0.6	0.7	1.4	24.5	
Full scale control: during Olympics (8–23 Aug 2008)	12 Aug 2008, 14 Aug 2008, 16 Aug 2008, 18 Aug 2008, 22 Aug 2008	Mean	1.1	96.1	3.1	1.3	2.7	2.9	71.9	5.5
		SD**	0.3	7.6	0.9	0.4	1.0	0.8	16.8	2.0
Between Olympics and Paralympics (24 Aug 2008–6 Sep 2008)	25 Aug 2008, 27 Aug 2008, 28 Aug 2008, 29 Aug 2008, 4 Sep 2008, 5 Sep 2008	Mean	1.4	112.8	7.9	2.0	3.9	3.8	63.0	6.0
		SD**	0.3	9.8	2.3	0.5	1.0	1.2	20.7	1.1
Full scale control: during Paralympics (7–19 Sep 2008)	8 Sep 2008, 9 Sep 2008, 10 Sep 2008, 11 Sep 2008, 18 Sep 2008, 19 Sep 2008	Mean	1.4	154.3	6.9	2.2	4.6	4.6		6.5
		SD**	0.4	17.0	2.4	0.6	1.2	1.1		1.6
Post Olympics (20–27 Sep 2008, 6 Oct 2008)	22 Sep 2008, 25 Sep 2008, 26 Sep 2008, 6 Oct 2008	Mean	1.4	170.0	5.2	1.7	4.4	4.1	105.7	6.1
		SD**	0.7	13.0	1.7	0.6	1.6	1.4	26.4	2.3
National holidays (28 Sep 2008–4 Oct 2008)	28 Sep 2008, 30 Sep 2008, 2 Oct 2008	Mean	2.0	154.4	10.4	2.8	5.2	4.7	124.2	8.9
		SD**	0.4	26.2	2.8	0.6	0.9	1.3	9.5	1.5

* X+E: xylenes + ethyl benzene. ** SD: Standard deviation.

ACPD
9, 12857–12898, 2009

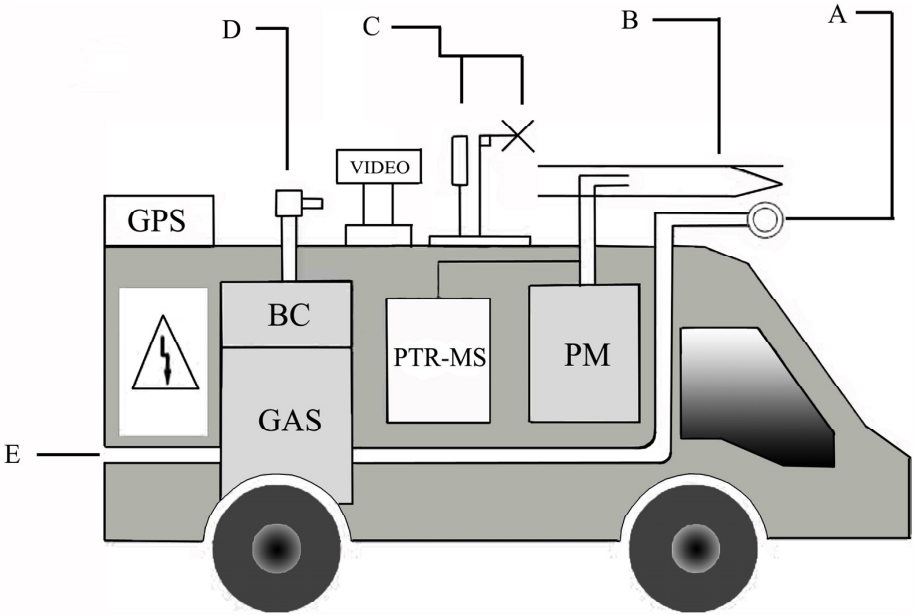

Fig. 1. Overview of mobile laboratory construction in Peking University. (A) gas inlet (B) aerosol and VOC_s inlets (C) wind speed, wind direction, relative humidity, temperature and pressure sensors (D) BC inlet with $PM_{2.5}$ cyclone (E) outlets of gas and aerosol instruments.

ACPD
9, 12857–12898, 2009

Fig. 2. Map of the city of Beijing. The 4th Ring Road was chosen as the sampling route and was equally divided into sixteen road lines colored by blue and red. The red plots show meteorological stations and place where traffic speed was record. (Version: Google map 2009).

ACPD
9, 12857–12898, 2009

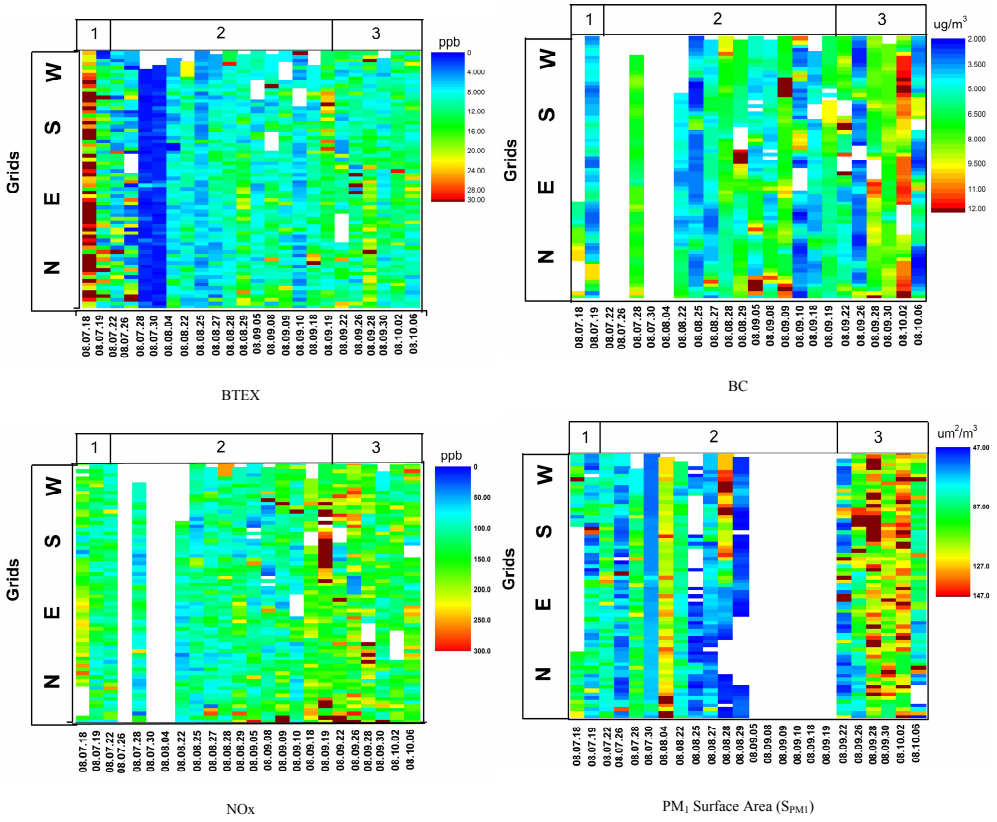

Fig. 3. Temporal and spatial distribution of the concentrations of BTEX, NO_x, and BC , and PM_1 surface area (S_{PM_1}) along the 4th Ring Road of Beijing, covering from pre-control to post-control periods. The number 1, 2, 3 represent different periods with regard to traffic control policy changes, 1: before full scale control (before 20 July); 2: with full scale control (20 July–19 September); 3: post Olympics (after 20 September). The letters N, E, S, and W represent the north, east, south, and west sections of the 4th Ring Road.

ACPD
9, 12857–12898, 2009

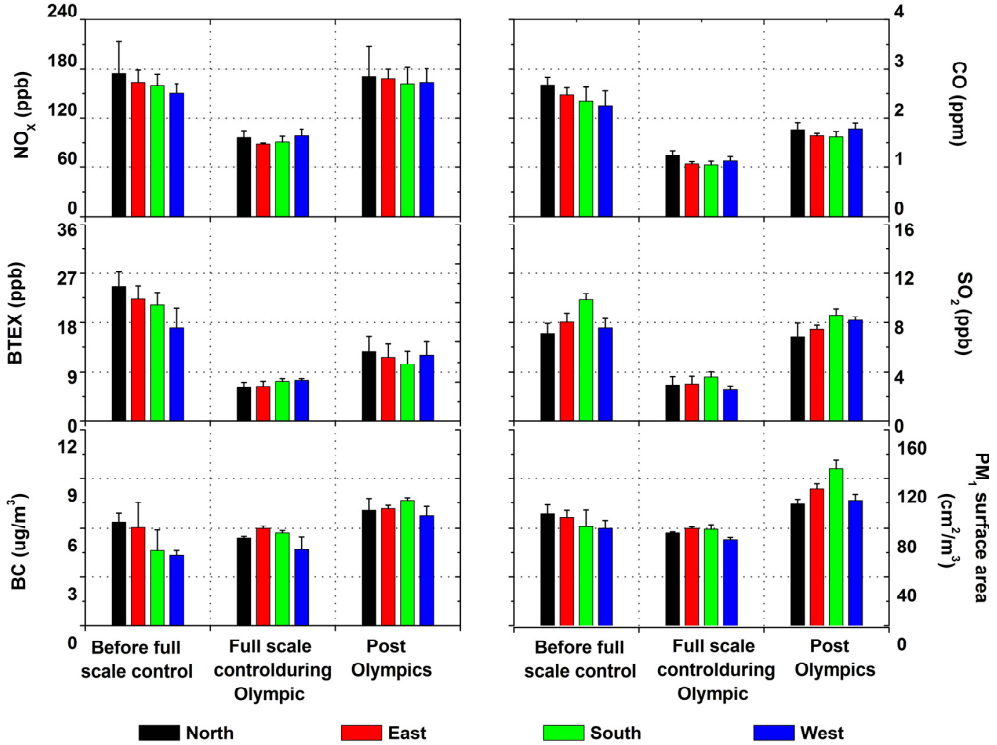

Fig. 4. The spatial variation of selected traffic-related pollutants (NO_x, CO, BTEX, SO_2, BC, and S_{PM_1}) on four directions of the 4th Ring Road (north, east, south and west) during periods of pre-full scale control (before 20 July), full scale control during Olympics (8–23 August) and post Olympics (after 20 September). The standard deviations represented the concentration differences of those pollutants on four road lines of each side as shown in Fig.2 during corresponding days of each periods.

ACPD
9, 12857–12898, 2009

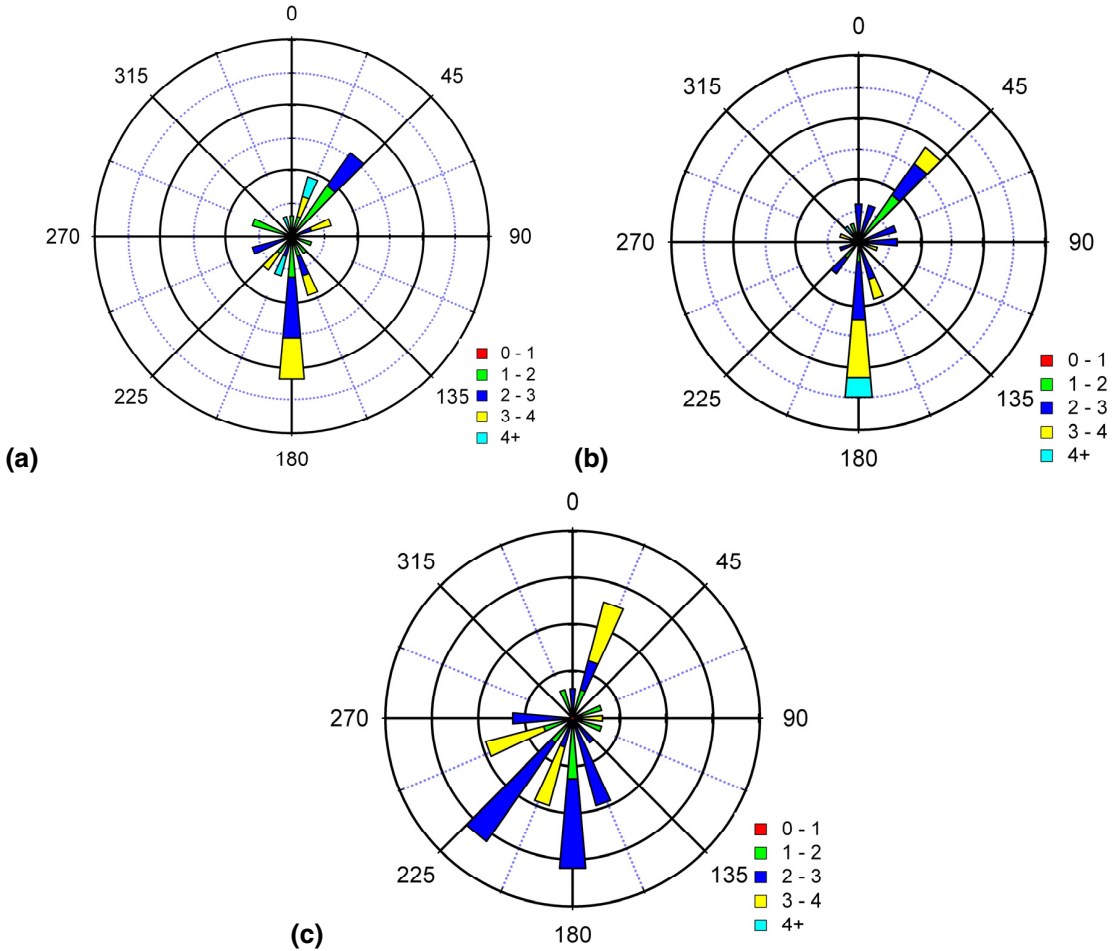

Fig. 5. Rose plots of wind measurements at **(a)** Haidian (NW), **(b)** Chaoyang (E), and **(c)** Fengtai (SW) meteorological stations during the period of on-road measurements.

ACPD
9, 12857–12898, 2009

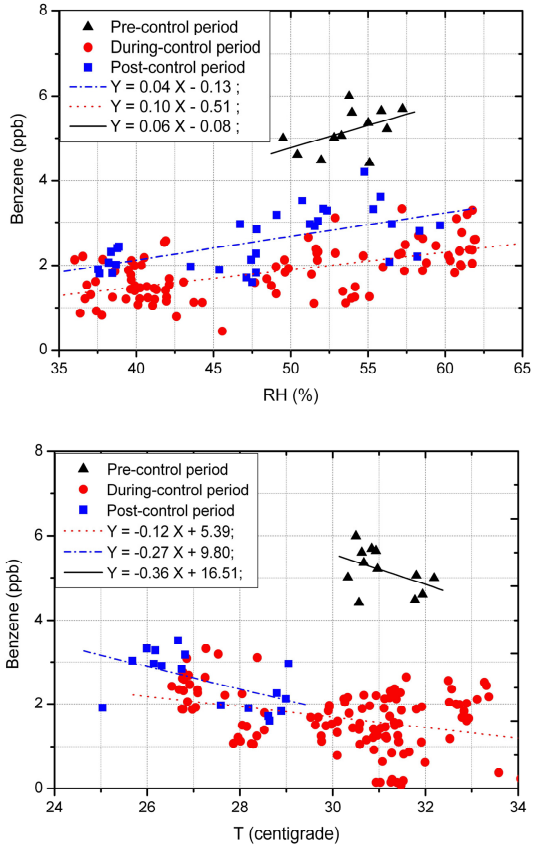

Fig. 6. Correlations between benzene and RH, *T* during the pre (before 20 July), during (20 July–19 September), and post (after 20 September) control periods. Each plot represented benzene concentrations of each road lines as shown in Fig. 2 corresponding to *T* and RH.

ACPD
9, 12857–12898, 2009

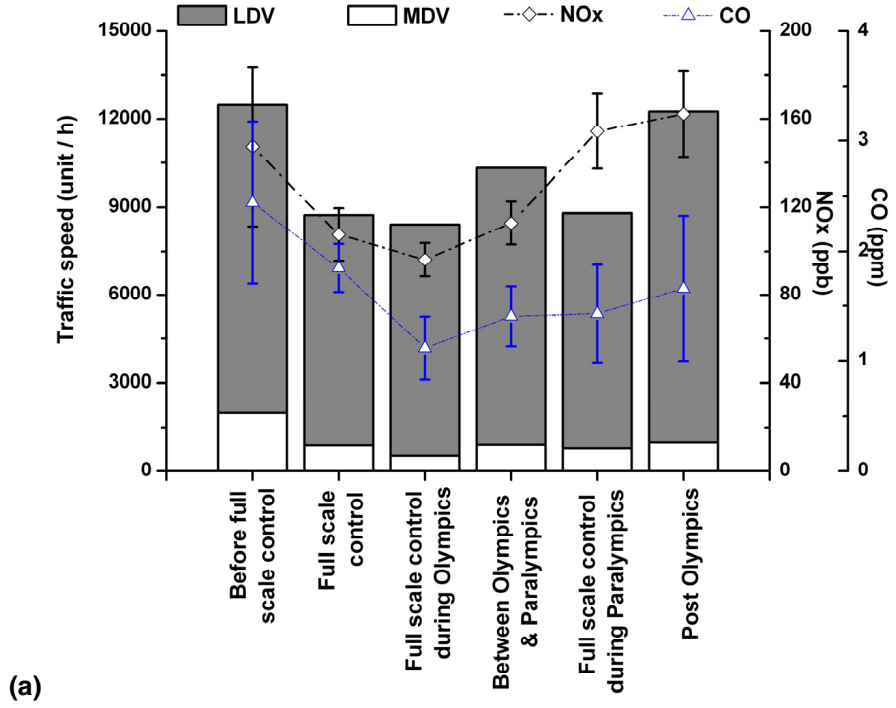

Fig. 7a. The traffic-related pollutants; **(a)** NO_x, CO, **(b)** BTEX, **(c)** BC and S_{PM_1}; separated into seven periods based on policy changes; before full scale control (before–20 July), Full scale control (20 July–7 August), Full scale control during Olympics (8–23 August), Between Olympics and Paralympics (24 August–6 September), Full scale control during Paralympics (7–19 September), Post Olympics (After–20 September); and corresponding vehicle numbers. The standard deviations represented the concentration differences of those pollutants during each cruise among each of corresponding periods.

ACPD
9, 12857–12898, 2009

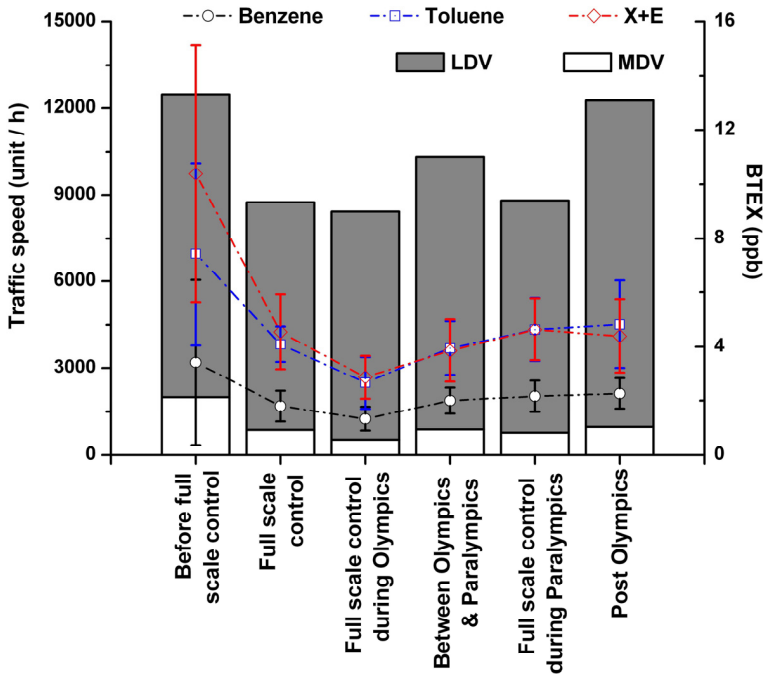

(b)

Fig. 7b. Continued.

ACPD
9, 12857–12898, 2009

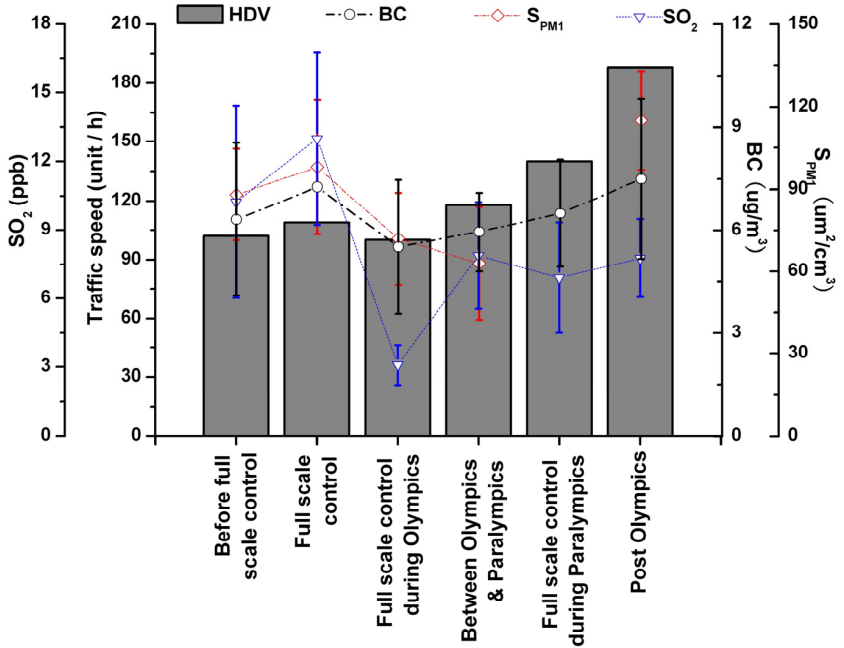

(c)

Fig. 7c. Continued.

ACPD
9, 12857–12898, 2009

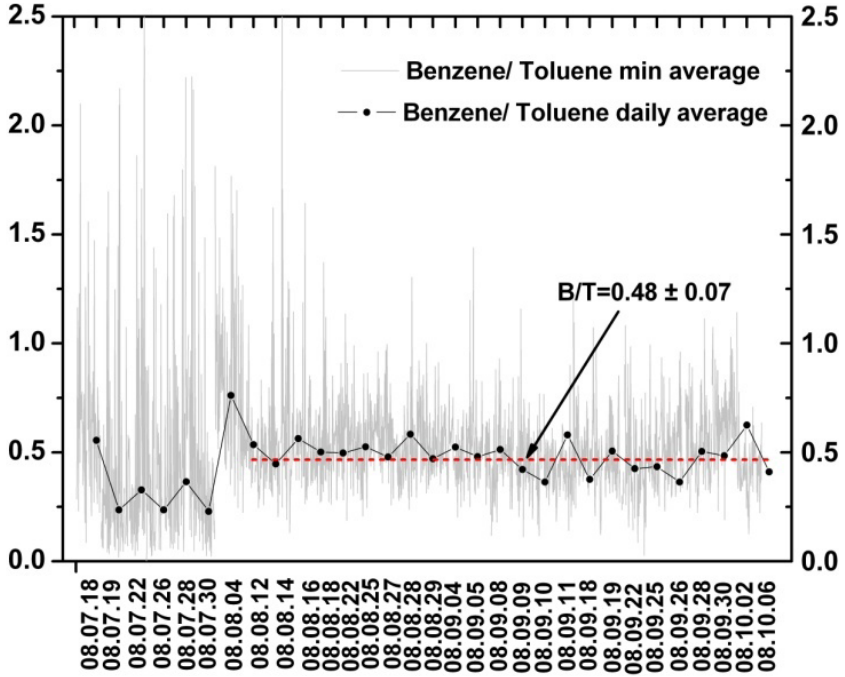

Fig. 8. The time series of benzene to toluene ratio on every cruise days. The light grey line represents real time minute average variation of on-road benzene/toluene ratio. The black symbol line shows daily average variation of on-road benzene/toluene on each cruise day. The red line shows the average benzene/toluene ratio in stable periods.

ACPD
9, 12857–12898, 2009

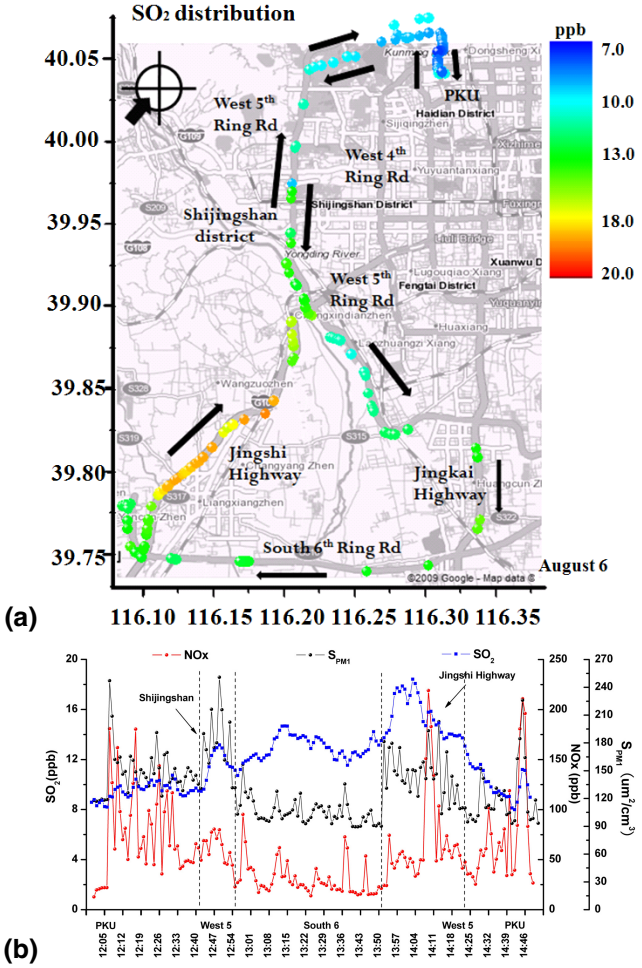

Fig. 9. SO_2 spatial distribution in **(a)** southwest of Beijing and **(b)** corresponding time serials variation. The prevailing winds were shown by arrow on top left of the map in **(a)** and the thin arrows in **(a)** represented the order of the cruise. The long dash line in **(b)** shows the range of local emission in Shijingshan district and regional transport in Jingshi Highway.

ACPD
9, 12857–12898, 2009